

Transmission intensity and the immunoepidemiology of bancroftian filariasis in East Africa

E.MICHAEL¹, P.E.SIMONSEN², M.MALECELA³, W.G.JAOKO⁴, E.M.PEDERSEN², D.MUKOKO⁵, R.T.RWEGOSHORA³ & D.W.MEYROWITSCH²

¹Department of Infectious Disease Epidemiology, Imperial College School of Medicine, London, UK, ²Danish Bilharziasis Laboratory, Charlottenlund, Denmark, ³National Institute for Medical Research, Dar es Salaam, Tanzania, ⁴Department of Medical Microbiology, College of Health Sciences, Nairobi, Kenya and ⁵Division of Vector Borne Diseases, Ministry of Health, Nairobi, Kenya

SUMMARY

Previous attempts to determine the interactions between filariasis transmission intensity, infection and chronic disease have been limited by a lack of a theoretical framework that allows the explicit examination of mechanisms that may link these variables at the community level. Here, we show how deterministic mathematical models, in conjunction with analyses of standardized field data from communities with varying parasite transmission intensities, can provide a particularly powerful framework for investigating this topic. These models were based on adult worm population dynamics, worm initiated chronic disease and two major forms of acquired immunity (larval-versus adult-worm generated) explicitly linked to community transmission intensity as measured by the Annual Transmission Potential (ATP). They were then fitted to data from low, moderate and moderately high transmission communities from East Africa to determine the mechanistic relationships between transmission, infection and observed filarial morbidity. The results indicate a profound effect of transmission intensity on patent infection and chronic disease, and on the generation and impact of immunity on these variables. For infection, the analysis indicates that in areas of higher parasite transmission, community-specific microfilarial rates may increase proportionately with transmission intensity until moderated by the generation of herd immunity. This supports recent suggestions that acquired immunity in filariasis is transmission driven and may be significant only in areas of high transmission. In East Africa, this transmission threshold is likely to be

higher than an ATP of at least 100. A new finding from the analysis of the disease data is that per capita worm pathogenicity could increase with transmission intensity such that the prevalences of both hydrocele and lymphoedema, even without immunopathological involvement, may increase disproportionately with transmission intensity. For lymphoedema, this rise may be further accelerated with the onset of immunopathology. An intriguing finding is that there may be at least two types of immunity operating in filariasis: one implicated in anti-infection immunity and generated by past experience of adult worms, the other involved in immune-mediated pathology and based on cumulative experience of infective larvae. If confirmed, these findings have important implications for the new global initiative to achieve control of this disease.

Keywords lymphatic filariasis, *Wuchereria bancrofti*, immunoepidemiology, transmission intensity, East Africa

INTRODUCTION

The role of transmission or exposure intensity on community patterns of infection and morbidity remains an unresolved question in human lymphatic filariasis epidemiology (1–5). This is despite field observations which suggest that the incidence of community infection and clinical morbidity may be associated with the degree of exposure to mosquitoes harbouring infective larvae (1–4) and laboratory studies which indicate that frequency of exposure to infective larvae can determine both the outcome of infection and the development of morbidity, most probably as a result of exposure-related changes in host immunity (6–10). The results of recent theoretical work, based on analyses of comparative age-infection data from field studies and mathematical models of host–parasite infection dynamics, also provide evidence for a

Correspondence: E.Michael, Department of Infectious Disease Epidemiology, Imperial College School of Medicine, Norfolk Place, London W2 1PG, UK

Received: 2 March 2001

Accepted for publication: 11 April 2001

transmission intensity-related acquisition of protective immunity in endemic communities (5). These studies clearly indicate the potentially central role that transmission intensity may play in infection, disease and immune processes but, because few studies have examined these processes simultaneously in the field, the precise relationships remain poorly understood. A better understanding of these inter-relationships has now become more urgent given the current global initiative for controlling transmission of filariasis by mass chemotherapy (11).

Interpretation of the results of previous field studies on the immunoepidemiological impact of community transmission intensity is further constrained by two additional factors. First, the use of different measures of entomological, infection and disease parameters, makes comparison between studies difficult (3). Second, past studies of the interrelationship between community transmission rates, infection and disease variables have largely been based on correlations between various entomologic indices of transmission, patent infection and disease rates (2–4). While important in uncovering the association between transmission intensity and community rates of infection and disease, this approach has rather less utility for investigating suggested mechanistic explanations for the observed copatterns of these variables. In particular, it is difficult to use such approaches to determine the contribution of host immunity to such patterns. By contrast, the use of mathematical models in conjunction with field data has helped to evaluate the population processes underlying patterns of infection and disease (12–15), including the impact of herd immunity on infection (5,16–19) and the interpretation of immunoepidemiological data (13,20)

Here, we describe the use of models for infection and disease (15,21) together with analyses of field data, to examine the mechanisms likely to underlie the interaction between community transmission intensity and the development of infection and disease in bancroftian filariasis. A particular focus of the study is the contribution of host immunity in regulating both infection and the development of chronic disease, and the role of community exposure rate in the generation of such immunity. The main dataset for the study is from two endemic villages in East Africa (22), but a comparison is also made with a previous study in the same region (23).

MATERIALS AND METHODS

The data

Given that the quantitative and qualitative relationships between transmission, immunity and the development of infection and disease are likely to vary with community

transmission intensity (5), we aimed to compare model fits to standardized indicators of age-patterns of infection and disease from at least two communities differing in mean overall transmission rates. Such parallel standardized entomological, parasitological and clinical data were recently collected from two communities in Tanzania (Masaika) and Kenya (Kingwede). Full details of the study are given in Simonsen *et al.* (22), and will only be summarized here. The infection parameter selected was measurement of microfilarial (mf) prevalence and intensity from 100 μ l finger-prick blood samples using the counting chamber technique (24). Blood sampling in both villages started at 21:00 h, and samples were collected from individuals using heparinized capillary tubes. Physical examination for hydrocele and lymphoedema was performed as previously described (25), except that all hydroceles \geq grade II (true hydroceles \geq 6.0 cm) and all lymphoedema/elephantiasis \geq grade I (loss of contour, pitting oedema) were included as hydrocele and elephantiasis, respectively. All examinations were carried out by an experienced clinician. To quantify community transmission rates in each village, mosquitoes were captured at weekly intervals from 50 randomly selected houses using CDC light-traps turned on at 18:00 h and turned off at 6:00 h the following morning. Mosquitoes were identified to species level, dissected and *Wuchereria bancrofti* larvae identified and counted (26). The Annual Transmission Potential [ATP, the total number of third-stage larvae (L3) to which an individual is exposed per year] was calculated according to Walsh *et al.* (27), and constitutes the exposure index representing the community transmission intensity in each village. *Anopheles gambiae*, *Anopheles funestus* and *Culex quinquefasciatus* were the three major vectors.

In addition to this primary dataset, models were also fitted to published data on age-patterns of microfilaria and chronic filarial disease in Tawalani, Tanzania, as described in McMahon *et al.* (23). This allowed a comparison with a community exposed to an even higher degree of transmission (ATP = 336.42) compared to Masaika (ATP = 99.68) and Kingwede (ATP = 10.28) in the same endemic area.

The model

The basic mathematical model used to describe the relationship between community transmission intensity and population age-patterns of infection and chronic disease essentially follows those of Chan *et al.* (15) and Norman *et al.* (21). However, to model the relationship between community transmission intensity (ATP), age-patterns of microfilaraemia prevalence and density, and pathology, we modified these earlier models in two directions.

Modelling the link between ATP and infection dynamics

The infection model used describes the changes in levels of the sexually mature adult worm population in the lymphatics and the mf population in the peripheral blood in a host population of constant size (15,21). Adult worms (W) in a host are acquired at a constant rate (the rate of gain of infection) by exposure to infective vectors. This rate increases linearly up to the age of 10 years and remains equal thereafter. Worms are lost through mortality at a per capita rate μ . Letting $MayL^*\psi h(a)$ represent age-specific ATP values, where May is the annual infective biting rate (AIBR) and L^* is the mean number of L3 per infected mosquito, and assuming a proportional relationship between ATP and the rate of gain of infection, the above formula easily allows for a simple link to be made between parasite transmission intensity and worm infection dynamics by the following equation describing the rate of change of worm burden by age:

$$dW/da = MayL^*\psi h(a)e^{-cl} - vW \tag{1}$$

where ψ is the coefficient of transmission which represents all transmission processes from the exit of third stage larvae from the vector to parasite establishment in the lymphatics (21). mf dynamics are related to the underlying transmission-worm burden dynamics by simply considering the rate of mf output in peripheral blood, M (appropriately scaled to reflect the number per blood sample), as a product of worm burden, W and per capita fecundity rate, α . mf are lost due to a natural death rate, b . The dynamics of mf counts in the model are then given by the equation:

$$dM/da = \alpha W - bM \tag{2}$$

As before, mean mf intensity in each age class is converted to prevalence at age a by using the negative binomial model relating mf intensity to prevalence (15).

Acquired immunity against infection can be considered to arise in two ways. While in both cases this immunity is assumed to develop at a rate, c , which is proportional to past experience of infection, I , the first model considers that the cumulative worm burden contributes to the experience of infection whereas, in the second model, experience of infection is a function of the cumulative rate of exposure to infective larvae. These models, designated as (a) and (b), respectively, are portrayed diagrammatically in Figure 1 (shaded portion). Model (a) reflects a general model of acquired immunity in helminth infections (15,20,28), while Model (b) immunity is not only directly related to transmission intensity, but also has been specifically implicated in antifilarial immunity, at least in animal infections (6–10). For both models, the underlying experience of infection, I , the parameter that gives rise to

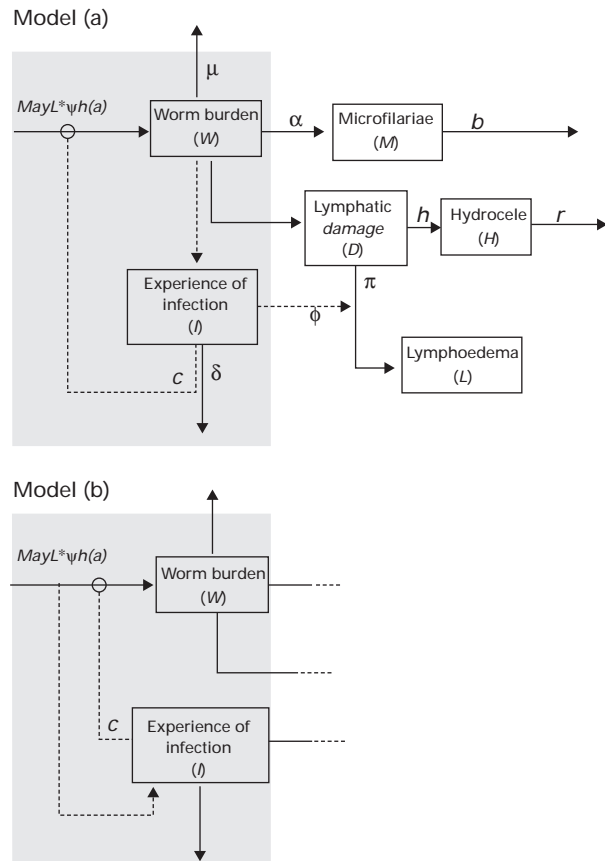


Figure 1 Diagrammatic representation of the structure of models described in the text. The shaded regions serve to highlight the different modes of development of immunity embodied by each of the two models studied. Note that the development of chronic disease is similar for each model and so not repeated in the figure for Model (b).

effective immunity in the model (20), decays at a rate δ , the rate of loss of immunological memory (Figure 1). These assumptions give the following equations for changes in the experience of infection with age for Model (a):

$$dI/da = W - \delta I \tag{3}$$

and for Model (b).

$$dI/da = MayL^*\psi h(a)e^{-cl} - \delta I \tag{4}$$

Models for chronic disease

As described in Chan *et al.* (15), these models recognize that chronic disease pathogenesis is fundamentally related to worm burden and associated lymphatic damage, exacerbated either by inflammatory reactions to secondary bacterial infections or by immunopathological reactions (29–32). The models begin with the central principle that

Table 1 Population variables, model parameters and default parameter values

Population variables	
W = adult worm burden	
M = microfilarial burden	
I = experience of infection	
D = proportion of individuals with lymphatic damage	
H = proportion of males with hydrocele	
L = proportion of individuals with lymphoedema	
Model parameters	
	Parameter values*
ϕ = coefficient of transmission	Estimated by model
μ = per capita mortality rate for adult worms	8 years
α = production rate of microfilaria per worm	120 per year
b = per capita mortality rate for microfilaria	1 year
h = rate of development of hydrocele due to lymphatic damage	Estimated by model
r = rate of resolution of hydrocele	Estimated by model
π = rate of development of lymphoedema due to lymphatic damage	Estimated by model
ϕ = immunological component of the development of lymphoedema	Estimated by model
c = rate of decrease in rate of infection with age as a result of immunity	Estimated by model
δ = rate of loss of immunological memory	Estimated by model

* Default values from Chan *et al.* (15) and Norman *et al.* (21).

all infected individuals develop worm-induced lymphatic damage, initially clinically asymptomatic, which is irreversible. All are at subsequent risk of lymphoedema, while males with lymphatic damage may also develop hydrocele. Assuming disease states to be a set of nonexclusive classes, the rate of development of each state can be modelled based on simple catalytic processes (15). Thus, the rate of development of lymphatic damage, D , assuming no resolution, is considered to be directly proportional to worm burden giving the following equation:

$$dD/da = W(1 - D) \quad (5)$$

Lymphoedema (L) is assumed to develop firstly at a constant rate π from direct lymphatic damage and secondary microbial infections, and secondly via immunopathological reactions at a rate (ϕ) that is proportional to the level of infection experienced (Figure 1). The different forms of immunity represented by Model (a) and Model (b) (Figure 1) allow examination of the relative importance of worm- versus infective larvae-induced immunopathological reactions in the progression of lymphoedema. Reactions to infective larvae have been shown to be important in disease development in animal models (6–8) and may underlie the reduction in acute adenolymphangitis episodes [thought to contribute to the development of chronic disease (30)] seen in transmigrants moving from an endemic area to an area of nontransmission (32). The present models will thus allow for the first time the explicit assessment of the likely impact

of this immunity on population patterns of chronic human filarial disease. Assuming no spontaneous resolution, the change with age in the proportion of individuals with lymphoedema is thus given by:

$$dL/da = (\pi D + \phi DI)(1 - L) \quad (6)$$

Finally, hydrocele in males is assumed to develop at a constant rate h with possible resolution at a constant rate, r , giving the equation:

$$dH/da = hD(1 - H) - rH \quad (7)$$

The link to worm dynamics in these formulations allows the explicit modelling (and examination) of the effect of variations in transmission intensity on observed community patterns of chronic disease. Figure 1 presents the structure of the models graphically while the various population variables and parameters of the models are summarized in Table 1.

Model fitting and interpretation

The present models allow inspection of different mechanistic explanations for the observed correlations between transmission intensity, immunity and community age-patterns of microfilaraemia and chronic disease. Since the mechanisms underlying these relationships are still unknown, one of the aims of this study is to discriminate between different suggested mechanisms by comparing the goodness of fit of competing models to the observed data

Table 2 Demographic characteristics, prevalence of microfilaraemia (mf) and clinical signs, and community transmission intensity in Masaika and Kingwede (22)

	Masaika	Kingwede	Statistics
No. of inhabitants (> 1 year)	950	1013	
Age range of participants	1–84 years	1–78 years	
mf prevalence (%)	211/848 (24.9)	22/825 (2.7)	Chi-squared test, $P < 0.001$
mf GMI (mf/ml)	16.4	0.8	<i>t</i> -test, $P < 0.001$
Hydrocele prevalence in males (%)	55/435 (12.6)	7/376 (1.9)	Chi-squared test, $P < 0.001$
Lymphoedema prevalence (%)	19/850 (2.2)	3/863 (0.3)	Chi-squared test, $P = 0.009$
ATP	99.68	10.28	

GMI, Geometric mean intensity. Hydroceles \geq grade II (25). Lymphoedema \geq grade I (25). Annual Transmission Potential calculated according to (27).

using the method of maximum likelihood to obtain the best-fitting model (and hence mechanism) for the given dataset (33,34). The method is based on finding the parameter estimates of each competing model that make the likelihood of observing the data as large as possible, followed by comparison of individual model likelihoods. The model giving the highest likelihood or equivalently the lowest minus log likelihood (and a good fit to the data) is considered to provide the best explanation for the data. A distinction is made between nested and non-nested models in model selection. A nested or hierarchical set of models is one in which a more complex alternative model (with additional parameters) reduces to a simpler model by setting the extra parameters equal to 0. Such models are discriminated using the likelihood ratio test, which has a chi-squared distribution with degrees of freedom equal to the difference in the number of parameters between the two models (33). When comparing non-nested models, we use the Akaike Information Criterion (AIC) for model discrimination, whereby the model with the smallest AIC value is selected (33). Given that model adequacy in this study is evaluated against the observed age-prevalences of microfilaraemia, hydrocele and lymphoedema in each study community, we fit the present models to (these) data by maximum likelihood assuming binomial errors (21).

RESULTS

Overall patterns of filariasis transmission, infection and disease in the two study communities

Table 2 summarizes population demographics, prevalence of microfilaraemia and chronic filarial disease, and estimates of the ATP in Masaika and Kingwede. The results clearly show, from the estimated ATP values, that parasite transmission was some nine times greater in

Masaika. Prevalence and mean intensity of microfilaraemia and of both hydrocele and lymphoedema were also significantly higher. The geometric mean mf count was also significantly greater (almost 20 times) in the higher transmission community. The observed prevalences of microfilaraemia and chronic disease were very low in Kingwede, only 22/825 individuals being positive for microfilaraemia and seven of 376 males and three of 863 individuals being positive for hydrocele and lymphoedema, respectively. The prevalence of lymphoedema in Masaika, though higher than in Kingwede, was also relatively low (19/850 individuals). The population demographics given in Table 2 indicate that neither sample size differences, nor variations in the age of study subjects are likely to influence these observed differences.

Fitting of transmission models to field data

The infection model described here, although describing changes in mean worm burden (Equations 1 and 2), was fitted using microfilariae prevalence data (see above). This therefore necessitated quantifying the relationship between mf prevalence and mean intensity (15). Figure 2 plots this relationship derived from comparable age classes in Masaika and Kingwede. The curve in the graph also shows that a negative binomial model of the form:

$$P_a = 1 - [1 + M_a/(k_0 + k_1 M)]^{-(k_0 + k_1 M)} \quad (8)$$

where P_a is the prevalence in age class a and M_a is the average mf count in age class a , provides a good fit to these data. Note that the parameter k (the degree of aggregation) is a linear function of mf count (see legend to Figure 2 for the estimated parameter values and details of fitting the model by maximum likelihood). This estimated relationship was then used to predict age prevalence curves from the corresponding mean mf intensity changes described by

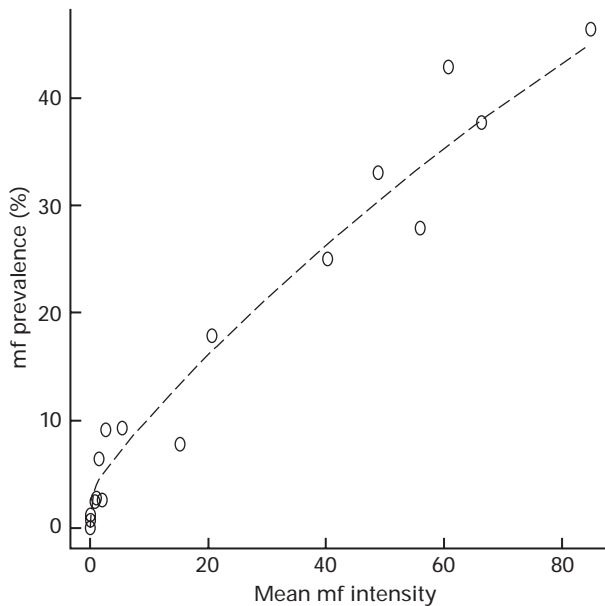


Figure 2 Plot of prevalence of microfilaria (mf) in blood versus mean mf counts. Data (circles) represent aggregates from corresponding age-classes in Masaika and Kingwede (see text). The line shows the fit of the negative binomial model (Equation 8) described in the text with parameter values and best-fit statistics: $k_0 = 0.0077$, $k_1 = 0.00093$, log likelihood = -524.93 , chi-squared (over model with constant k) = 34.18 , d.f. = 1 , $P < 0.001$

the infection model (Equation 2), thus allowing model fits to the observed mf age-prevalence data.

Figure 3 depicts the age patterns of microfilaraemia and chronic disease observed in Masaika. Both the prevalence and mean intensity of microfilaraemia show an increase with age with a slight tendency for both to plateau among the oldest age-classes (22) (Figure 3a,b). By contrast, prevalence of both hydrocele in males and lymphoedema increase linearly with age (Figure 3c,d), although the age-pattern of the latter condition is markedly variable, probably due to the small number of patients ($n = 19$) (Figure 3d).

The maximum likelihood analysis of the fit of the transmission model for infection (Equations 2 and 3) to the

Table 3 Results of model fits to infection data from Masaika

	ψ	c	Log likelihood	P^*
(a) No immunity	0.00067	–	– 432.68	
(b) With immunity [model (a)]	0.00067	0	– 432.68	NS
(c) With immunity [Model (b)]	0.00067	0	– 432.68	NS
Saturated model			– 428.47	

P^* is given with respect to the simplest model, i.e. Model (a).

mf age-prevalence data from Masaika for the given ATP of 99 is shown in Table 3. The results indicate that the observed data are best fit by the model with no immunity (model not significantly different from the saturated model). Addition of either type of immunity (worm- or infective larvae-induced) did not improve the fit of the basic model (Table 3). Allowing immunity to decay also did not improve the fit (results not shown). Figure 3(a) plots the predictions of the best-fit model against observed prevalence data, and shows good correspondence with the curve falling within the standard errors of most of the data. This plot shows prevalence increasing until around the age of 35 years and leveling off thereafter. Figure 3(b) shows that this model also corresponds well with the data on mean mf count, which although more variable, show a similar age-pattern of increase of infection.

The results of the maximum likelihood fits of the models for chronic disease (Equations 5–7) are given in Table 4, and indicate that, for hydrocele, the simplest model with no resolution is not significantly different from the saturated model and hence already an adequate descriptor of the data. Similarly, for lymphoedema, the simplest model with no immunologically induced development of disease is not significantly different from the saturated model (Table 4), although clearly this conclusion is limited by the evident variability in the data (Figure 3d). These results imply that, in Masaika, development of chronic disease is simply an outcome of lymphatic damage caused by worms, and in the case of lymphoedema apparently has no immunological involvement. The most parsimonious models for hydrocele

Figure 3 Fitted models for infection and disease prevalence in Masaika. (a) and (b) show the fits of the infection model for an ATP of 99 (Table 3) to microfilaria (mf) prevalence and mean intensity by age, respectively; while (c) and (d) portray disease model fits (Table 4) to the observed age-patterns of hydrocele and lymphoedema in the community. Symbols in the graphs denote the data in each age-class while the bars represent the corresponding standard error of each data point. Solid lines in the graphs depict the best-fit models (Tables 3 and 4) for each infection/disease variable; whereas the dashed and dot-dashed lines in (d) simulate the prevalence of lymphoedema that would be expected if some immunological involvement were to occur in disease development. The dashed line shows the expected prevalence if immunopathology occurs as a result of immunity to adult worms while the dot-dashed line represents the corresponding prevalence when immunologically induced development occurs as a result of immunity to infective larvae. The simulations are carried out for a similar value of ϕ , the rate of immunopathological development (Equation 6), in each case, and illustrate that for a given rate (or strength of immunity) disease development as a result of immunopathological reactions to adult worms will be greater compared to that developing from immunity to infective larvae (see text for an explanation for this result). Standard errors for the prevalence data were calculated using the normal approximation to the binomial distribution.

and lymphoedema is shown in Figure 3(c,d). They indicate a good fit between model and data for hydrocele and, overall, also for lymphoedema (Figure 3d). As noted by Chan *et al.* (15), the parameter values for the rates of

development of hydrocele and lymphoedema listed in Table 4 can be interpreted as the risks of developing each of these diseases per worm-year of infection experienced. The present results indicate these risks in Masaika to be 1.0%

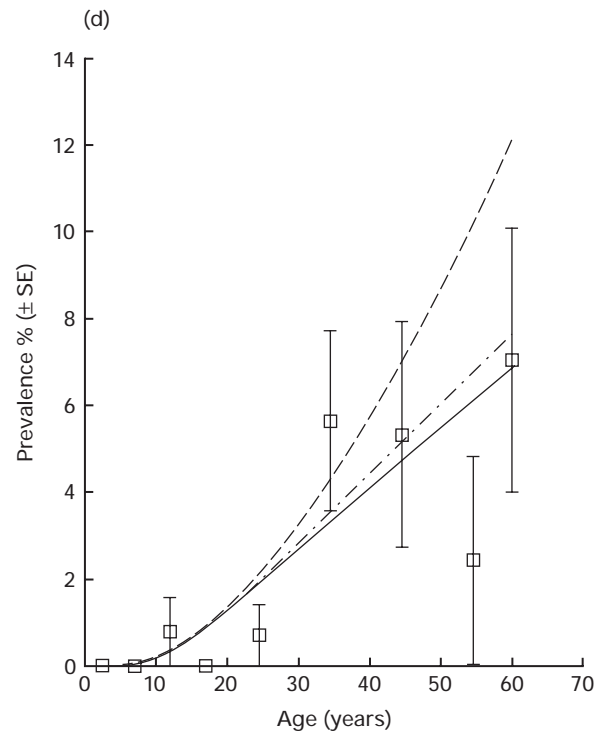
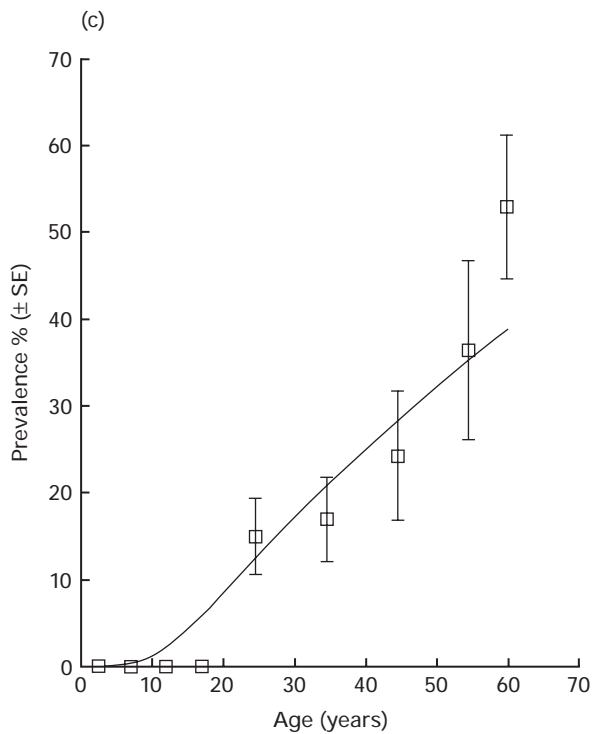
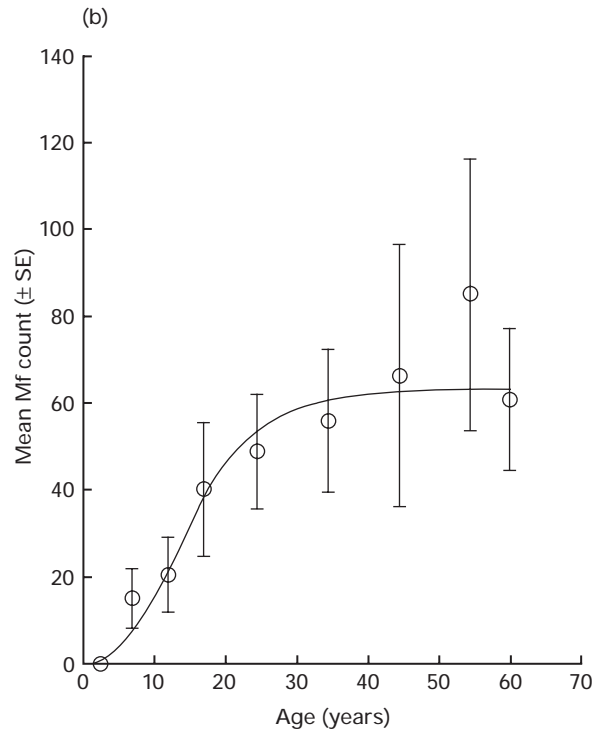
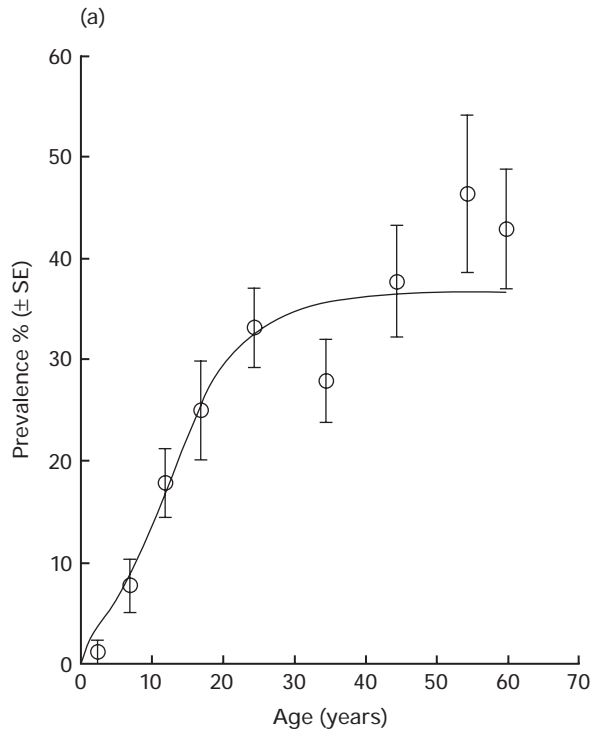


Table 4 Results of model fits to disease data from Masaika

Model	h	r	Log likelihood	P^*
(1) Hydrocele*				
(a) No resolution ($r = 0$)	0.01004	–	– 118.95	
(b) With resolution ($r \geq 0$)	0.01004	0	– 118.95	NS
(c) Saturated model			– 112.68	
Model	π	ϕ	Log likelihood	P^*
(2) Lymphoedema				
(a) No immune component ($\phi = 0$)	0.00146	–	– 80.38	
(b) With immune component ($\phi \geq 0$) (Model A)	0.00146	0	– 80.38	NS
(c) With immune component ($\phi \geq 0$) (Model B)	0.00146	0	– 80.38	NS
Saturated model			– 77.11	

P^* is given with respect to the appropriate simplest model, i.e Model (1a) and (2a).

per worm-year for hydrocele and 0.15% per worm-year for lymphoedema. These compare with 2.2% and 0.33% per worm-year, respectively, estimated by Chan *et al.* (15) for their South Indian study community, indicating that, on average, worm-induced pathogenesis in Masaika is one-half

of that established by the same disease model for the Indian community. This may indicate differences in infection estimation, regional differences in worm pathogenicity, host differences in the rate of developing disease from a given worm infection or even density dependence in *per capita*

Table 5 Parameter values of best fit models to infection and disease data from Kingwede

Model	ψ	c	Log likelihood	P^*
(1) Infection				
(a) No immunity (unadjusted Mf)	0.00006	–	– 90.07	< 0.05
(b) No immunity (adjusted Mf)	0.00095	–	– 160.80	< 0.05
Saturated model (unadjusted Mf)			– 85.31	
Saturated model (adjusted Mf)			– 142.99	
Model	h	r	Log likelihood	P^*
(2) Hydrocele				
(a) No resolution ($r = 0$) (unadjusted Mf)	0.03421	–	– 23.52	NS
(b) No resolution ($r = 0$) (adjusted Mf)	0.00390	–	– 23.93	NS
Saturated model			– 22.35	
Model	π	ϕ	Log likelihood	P^*
(3) Lymphoedema				
(a) No immune component ($\phi = 0$) (unadjusted Mf)	0.00585	–	– 17.07	NS
(b) No immune component ($\phi = 0$) (adjusted Mf)	0.00067	–	– 16.86	NS
Saturated model			– 15.27	

Model likelihoods compared with the maximum achievable likelihoods of the respective saturated models for unadjusted and adjusted data. Note that, unlike for infection, there is only one saturated model for disease. Likelihoods of models based on unadjusted and adjusted microfilarial counts are compared with the maximum achievable likelihood of the appropriate single saturated model in each case. P^* indicates goodness of fit of each model with the corresponding saturated model. NS = not significantly different from saturated model. $P < 0.05$ indicates a poor fit to data.

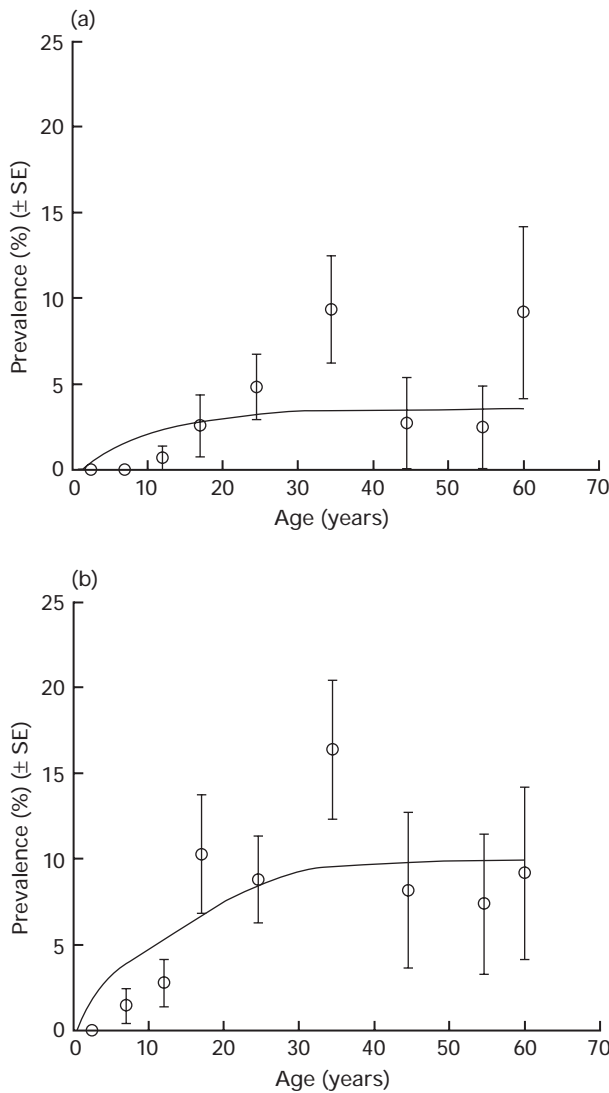


Figure 4 Fits of the infection model to (a) unadjusted and (b) adjusted microfilaria (mf) age-prevalence data from Kingwede. The models in each case are based on an ATP value of 10. Parameter values and details of model fits are as given in Table 5. See text for explanations for the adjustment of mf counts carried out in (b); symbols and bars are as described in the legend to Figure 3.

worm pathogenicity, such that the effect per worm is related to worm burden (see below).

Figure 3(d) also simulates the impact of immunological involvement in the age-prevalence of lymphoedema in Masaika. The results illustrate firstly that any addition of immunologically induced lymphoedema to physically induced disease ($\phi > 0$) irrespective of whether generated by experience of adult worms [Model (a) immunity] or infective larvae [Model (b) immunity] would disproportionately increase the prevalence of disease in the older age groups. Second, for the same rate of immunopathological

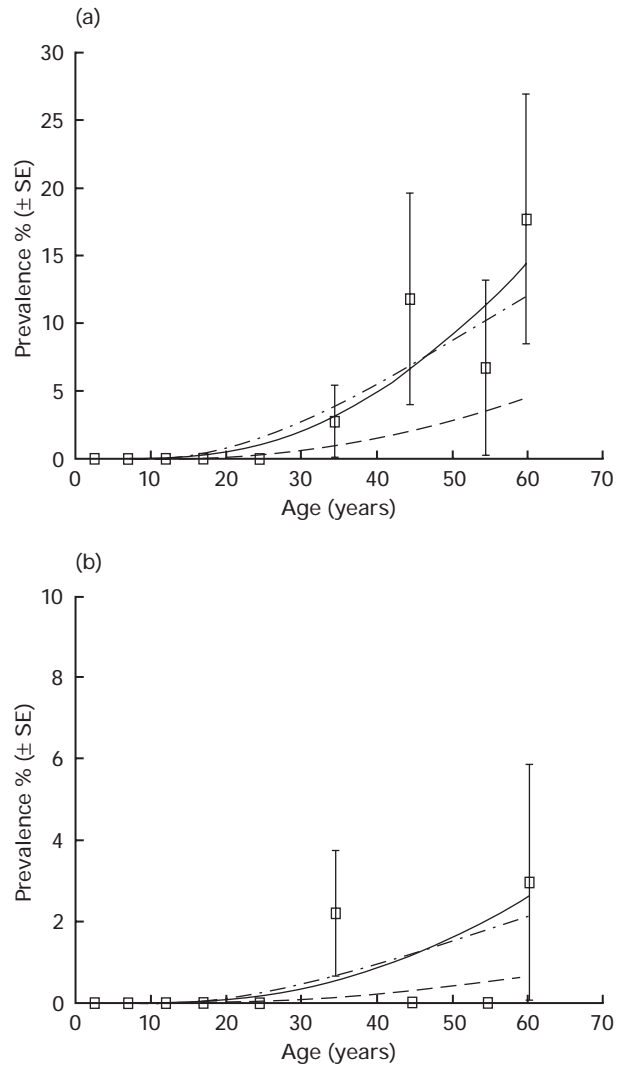
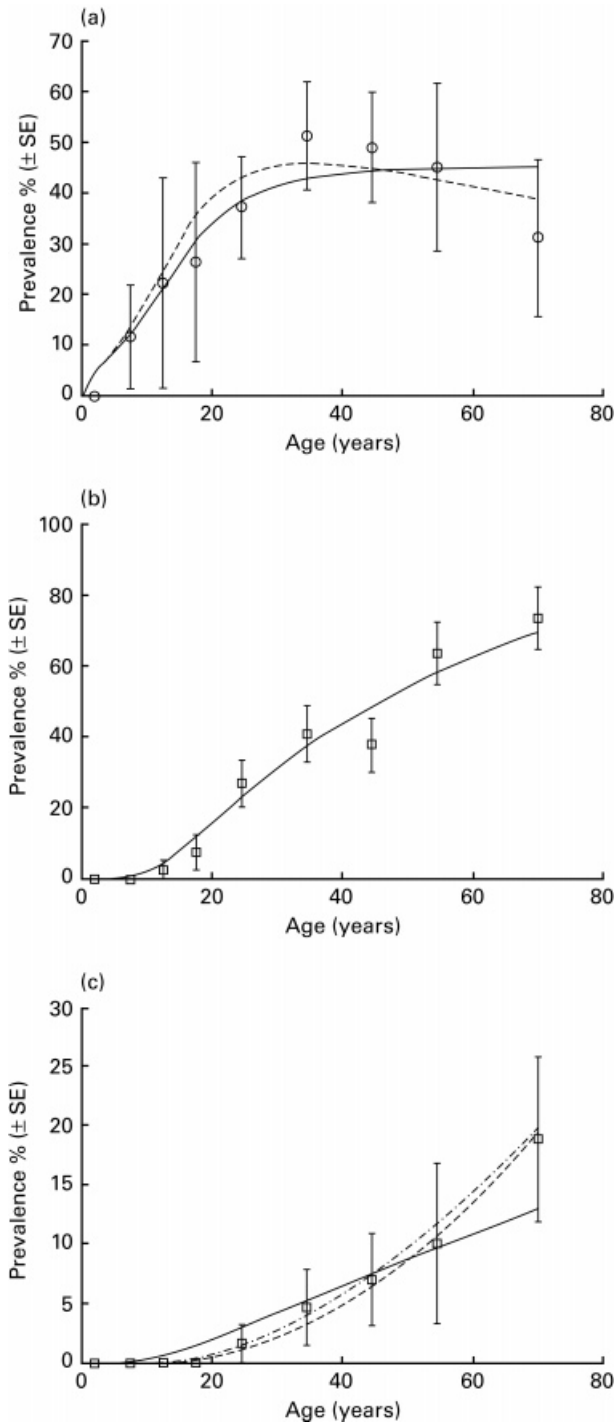


Figure 5 Fits of the disease model to age-prevalences of (a) hydrocele and (b) lymphoedema in Kingwede. Symbols and bars as described in the legend to Figure 3. The solid line in each graph refers to the respective best-fit model based on unadjusted microfilaria (mf) counts (see Table 5 and text), while the dot-dashed line portrays the fit of the corresponding model based on adjusting the mf count as described in the text for each disease. The dashed line in each graph depicts the predictions of the respective unadjusted models for hydrocele and lymphoedema in Kingwede based on the parameter values obtained for the best-fit disease models in Masaika (Table 4).

development (e.g. $\phi = 0.0001$ in the present simulation), development of lymphoedema from immunological reactions to adult worms [Model (a) immunity] will lead to higher prevalences of disease than those resulting from immunopathological reactions to infective larvae (Figure 3d). This results from the higher level of cumulative infection experience that develops due to worm burden in the model (resulting largely from the relatively long

average worm life span) compared to the realized level arising from the corresponding experience of infective larvae.

Table 5 and Figures 4 and 5 summarize the fits of the transmission models to the data from the lower transmission intensity (ATP approximately 10) village of Kingwede.



Two major problems impeded the statistical fitting and direct interpretation of the models for these data. The first concerns the degree of variability in both the infection (Figure 4a) and disease data (Figure 5), which probably reflects the low prevalences of microfilaraemia and chronic disease in this community. The second problem is related to the low mean mf counts in the community. Because mf detection using relatively small blood volumes is notorious for missing infection when overall infection levels in the community are low (5,35,36), interpretation of the model may reflect an artifact of blood sampling variation rather than actual parasite population dynamics. Sampling variability will clearly also hamper comparability of the results with those from Masaika. We have addressed this problem by correcting for the prevalence and level of infection missed in Kingwede, using the prevalence that may be detected in the community were a more sensitive test be used. The results of applying one such test based on parasite antigen detection are given in detail in Simonsen *et al.* (22). These indicated that up to approximately six times more individuals (a community antigen positivity rate of 16.5%) may show signs of infection in Kingwede compared to a prevalence of only 2.7% based on mf detection (Table 2). If we consider the former value to be nearer the likely mf prevalence, we can use Equation 8 also to estimate the likely mean mf intensity in the community. The result suggests that a correction factor of approximately 6.5 would require to be applied to the measured mean mf counts.

The results of model fits to the Kingwede data are given in Table 5. Apart from identifying the most parsimonious model for each infection and disease variable, they also highlight how variability in infection detection might lead to misleading conclusions regarding population dynamics. For example, although as in Masaika, the most parsimonious model for infection, whether based on unadjusted or corrected mf counts, is one where there is no immunity, the

Figure 6 Fitted models for infection and disease prevalence in Tawalani. (a) Showing the fits of the infection model for an ATP of 336 (Table 6) to microfilaria (mf) age-prevalence while (b) and (c) portray the disease model fits (Table 7) to the observed age-patterns of hydrocele and lymphoedema in this community. Symbols and bars in each graph are as described in the legend to Figure 3. In (a), the solid line depicts the predictions of the infection model with no immunity, while the dashed line portrays the fit of the Model (a) (to adult worms). In (c), the solid line is the prediction of the model with no immunity while the dashed and dot-dashed lines represent Models (a) and (b), respectively. The graph shows that the latter may be the best-fitting model for this dataset, implicating a role for immunopathology as a result of immune reactions to infective larvae in the development of lymphoedema in an high transmission community. The solid line in (b) is the best-fit hydrocele model summarized in Table 7.

Table 6 Results of model fits to infection data from Tawalani

	ψ	c	Log likelihood	P^*	AIC
(a) No immunity	0.000156	–	– 188.19		
(b) With immunity (Model A)	0.000199	0.01993	– 187.03	~0.10	378.06
(c) With immunity (Model B)	0.000177	0.09536	– 187.99	NS	379.98
Saturated model			– 183.60		

P^* is given with respect to the simplest model, i.e. Model (a).

value of the transmission coefficient (0.00006) obtained for the model based on the uncorrected mf counts is an order of magnitude smaller than that obtained for the best-fit infection model in Masaika ($\psi = 0.00067$), suggesting that the probability of worm establishment in the host lymphatics increases with transmission intensity. By contrast, the coefficient of transmission estimated by the model based on corrected mf counts is not only comparable to that estimated for Masaika, but may even be slightly higher (Table 5). Such (negative) density-dependence regulation of larval transmission/establishment with increasing intensity of transmission is likely to be a more plausible outcome in vector-borne infections (37). These contrasting interpretations clearly underscore the significance of efficient parasite detection in studies of filariasis infection dynamics, and indicate the crucial importance of addressing this problem when interpreting data from different studies and sites. The most parsimonious models for unadjusted and adjusted mf prevalence data are plotted in Figure 4(a,b), and show a rise to a plateau around ages 40–45 years in both cases (better observed for the adjusted data). The later leveling of infection in Kingwede compared to Masaika (Figure 3a) accord with the results of simple immigration-death models for helminths (28), which predict that, all else being equal and in the absence of immunity, the age at which an infection reaches a plateau in the host population increases as the intensity of transmission decreases. The results thus indicate that the observed mf prevalence differences between Masaika and Kingwede are simply a direct function of differences in the mean parasite transmission intensity between the two villages, uncomplicated by any effects due to the acquisition of immunity.

Although the results need to be viewed cautiously because of the low numbers of diseased individuals and consequent high variability in the data (Figure 5), the analysis presented in Table 5 nevertheless highlights two issues of biological interest regarding the development of chronic disease in Kingwede. First, the results indicate that the processes underlying chronic disease evolution in this community are qualitatively similar to those governing

disease development in Masaika. Thus, for both hydrocele and lymphoedema, the most parsimonious model, whether based on unadjusted or corrected mean mf density, is also the simplest one in which the respective diseases develop irreversibly as a consequence of lymphatic damage caused by worms (Table 5). This suggests, as with infection, that the observed differences in disease rates between the two communities (Table 2 and Figures 3c,d and 5a,b) are also principally the consequence of transmission-related variations in worm burden.

The results in Table 5 and the model predictions in Figure 5 also illustrate how variability in infection detection may influence the analysis of processes underlying chronic disease development. This can be seen by comparing the parameter values for the rates of development of hydrocele (h) and lymphoedema (π) as a function of worm burden for the unadjusted and adjusted mf models, respectively (Table 5). For each disease, although the predictions from both models fit the respective data well (Figure 5a,b), the rates are an order of magnitude higher for the unadjusted model. The estimated parameter values for the unadjusted models are also significantly higher than the corresponding values obtained for Masaika (Table 4), apparently suggesting, as shown in Figure 5(a,b) (solid line versus dashed lines), that the risk of disease development per worm is significantly higher in the lower transmission community. The importance of efficient detection of infection, however, is demonstrated by the values obtained using the mf adjusted model which, in contrast to the first model, indicates a significantly lower risk of disease development per worm compared to that estimated in Masaika (Table 5). Because the model based on mf adjustment may be considered to be a more plausible for disease in Kingwede, and, as both study communities are from the same coastal East African transmission focus (only some 80 km apart), this raises the important possibility that per capita worm pathogenicity in filariasis may be related to the number of worms carried by the host, such that worm-induced physical damage may increase disproportionately (i.e. more than additively) with increasing worm burden.

Table 7 Results of model fits to disease data from Tawalani

	h	r	Log likelihood	P^*	AIC
(1) Hydrocele*					
(a) No resolution ($r = 0$)	0.02033	–	– 127.37		
(b) With resolution ($r \geq 0$)	0.02033	0	– 127.37	NS	
Saturated model			– 124.18		
	π	ϕ	Log likelihood	P^*	AIC
(2) Lymphoedema					
(a) No immune component ($\phi = 0$)	0.00124	–	– 45.19		
(b) With immune component ($\phi \geq 0$) (Model A)	0.00027	0.00026	– 44.07	NS	92.14
(c) With immune component ($\phi \geq 0$) (Model B)	0.00001	0.00197	– 43.97	~0.10	91.94
Saturated model				– 42.92	

P^* is given with respect to the appropriate simplest model, i.e Model (1a) and (2a).

Comparison of results with a high transmission community

The lack of evidence for an epidemiological impact of acquired immunity may reflect the fact that transmission intensity in both study communities is below the threshold required to induce significant immunity (5). Here, we test this hypothesis by fitting the models to comparable age-prevalence data from a study site (Tawalani) in the same endemic focus shown previously (23) to have a significantly higher community transmission intensity (as measured by the ATP). Transmission was by the same mosquito species, and entomological and clinical variables were measured using essentially similar methods to those in the present study, except that microfilariae were counted in 100 μ l blood samples after the diethylcarbamazine (DEC) day provocative test. Overall, ATP, mf, hydrocele (\geq stage 2) and lymphoedema prevalences were 336, 28.3% (104/367), 23.3% (45/193) and 3.3% (12/367) respectively, in Tawalani, i.e. significantly higher values than in the present study sites (Table 2).

A problem with using the mf data from the Tawalani study is that, although the effect on prevalence is small, the day provocative test on average tends to yield lower counts compared to those obtained using night-time finger-prick blood sampling (38). Comparability with the data from the present study therefore required the transformation of the mf data from Tawalani to reflect enumeration based on night-time blood samples. Two kinds of information are needed to accomplish this: (i) the proportional difference in mean counts obtained using the two methods, and (ii) the statistical relationship between mean intensity following transformation and prevalence of microfilaraemia. The first

was obtained using the night-time finger-prick (100 μ l)/ counting chamber method to resample a group of individuals studied originally by McMahon *et al.* (23). Although there was a time gap of nearly 15 years, analysis (not shown) indicated that there may be up to a 10-fold difference between the counts that was independent of the time factor (39). We therefore convert the mf intensity data from Tawalani here by a factor of 10. The second requirement was addressed by determining the relationship between mf prevalence and intensity using the converted mean counts, which again showed a good fit to the negative binomial model, with the parameter k being a linear function of the mean (Equation 8 with parameter values: $k_0 = 0.01317$ and $k_1 = 0.00128$).

Figure 6(a) plots the prevalence of microfilaraemia by age class in Tawalani, and indicates a steady increase in infection within the community to a peak at age 35 years followed by a subsequent decline ($P = 0.05$) thereafter. A feature is the relatively high degree of variability in the data, especially among the teenage and oldest age classes. The results of fitting the infection model (based on an ATP value of 336) are given in Table 6, and show that the model incorporating immunity to adult worms [Model (a)] may provide the best fit to these data, although this is at the 10% level of significance in comparison with the basic no-immunity model and is only just better than the model with immunity to infective larvae. Comparison of the model predictions (curves) in Figure 6(a) shows that this model also provides a qualitatively better fit to the data (compared to the basic model), especially within the later age groups.

The corresponding analyses of the disease models are shown in Table 7, and demonstrate that for hydrocele the

most parsimonious model is again the simplest one with no resolution but where the rate of disease development due to physical damage by worms is double that estimated for Masaika (Table 4). Figure 6(b) shows the excellent correspondence with the observed data. The fitting of the disease model to the lymphoedema data indicates that some immunological involvement in addition to worm-induced lymphatic damage is required to best describe the development of the disease in this higher transmission community (Table 7). The results also demonstrate that the best fitting model here is the one where immunity is to infective larvae [Model (b)] rather to adult worms [Model (a)], although this is significant at only the 10% level in comparison with the basic model and the difference between the two immunity models is slight (compare dashed lines in Figure 6c).

DISCUSSION

The models derived here are based on a previous deterministic model for filariasis infection and disease developed and validated against data from a community in Southern India (15,21). The central assumption of these models is that the prevalence of microfilaraemia and chronic disease in an endemic community is ultimately a function of adult worm load, which reflects current views regarding infection dynamics and the pathogenesis of chronic disease in lymphatic filariasis (31). The role of antifilarial immunity in this new paradigm is to moderate the rate of acquisition of worms with age and to influence the development of lymphoedema arising initially from worm-induced damage to the lymphatics (15,31). More precisely, the effect of acquiring immunity is considered to be negative for infection but positive for the development of lymphoedema. The contribution of the present work is (i) to link explicitly the basic model to parasite transmission intensity, as measured by the ATP, which for the first time provides a comprehensive framework for investigating the postulated mechanisms linking filarial transmission intensity, infection and disease in endemic communities; and (ii) to incorporate and investigate the likely impact of two types of parasite immunity, one reflecting accumulated experience of worms, the other reflecting cumulative exposure to infective larvae. These reflect the simplest forms of antifilarial immunity consistent with available information (6–10,15,20), although more complex mechanisms, particularly those related to antimicrofilaria immunity (8,13,40,41) may also need to be considered in future work.

The second stage of our analysis comprised fitting the derived models to data from communities with differing transmission intensities, and to use statistical analysis to discriminate between the models and hence the postulated

mechanisms linking parasite transmission with infection and disease in each community. The implicit hypothesis underlying this approach is that the development of infection and disease in each host community varies with the corresponding transmission intensity experienced. Indeed, a particular focus is to ascertain whether significant involvement of filarial immunity in regulating both infection and disease occurs only in communities with high transmission intensity, as suggested by previous work (5).

The analysis of model fits to field data has also emphasized the importance of applying uniform and sensitive indicators of infection when comparing epidemiological data between endemic communities. However, even when a uniform method is used, it is crucial that it should be of high sensitivity. In particular, the analysis indicates that estimates based on microfilaria detection in blood, especially when blood volumes are relatively small, may significantly underestimate infection levels in areas of low transmission and potentially lead to misleading conclusions regarding the pathogenesis of chronic disease. This was highlighted by the analyses of uncorrected data from finger-prick sampling of 100 μ l of blood that indicated higher worm pathogenicity in the low transmission community of Kingwede when the opposite is more likely to be true. This identifies a particular need for epidemiological studies to obtain more precise estimates of infection (both parasite prevalence and intensity) in endemic communities. Although measures of infection based on the more sensitive Og4C3-antigen detection test (TropBio[®] ELISA kit) were available for Masaika and Kingwede (22), their use was precluded by the inclusion of an upper cut-off level for antigenemia optical density (OD) values, which clearly interfered with more precise estimations of age-intensity patterns in these communities. Future studies based on such tests must address this aspect if antigenemia data are to be used gainfully in comparative epidemiological analyses.

Despite these caveats, the present mechanistic models for analysing comparative data from low, moderate and moderately high transmission communities within the same East African coastal endemic focus have produced new insights regarding the impact of transmission intensity variability on the development of infection and chronic disease as well as the effect of antifilarial immunity on these patterns at the community level. First, the fitting of the infection model supports recent views that acquired immunity to filarial infection is transmission driven and may only be manifest in communities of moderately high to high transmission intensity (5). Although the detection of anti-infection immunity in the field data for Tawalani was significant only at the 10% level, it is biologically relevant that this agrees with predictions of general models of

helminth immunity which incorporate a positive interaction between exposure and acquisition of herd immunity (17,28). An important implication of this result is that it suggests the likely existence of a transmission intensity threshold for the development of anti-infection immunity. Infection levels are related proportionately to transmission intensity below this threshold (at least $> ATP = 100$ for the present East African locale) whereas above it, immunity moderates infection levels, especially in older age-classes. The detection of such a threshold, and indeed more conclusive evidence for the manifestation of acquired immunity against filarial infection, will clearly require analysis of data from additional sites encompassing a wider spectrum (particularly higher) of transmission intensity than observed for Tawalani; this constitutes a priority in our work in this area.

Although the low numbers of disease patients and the consequent high variability in the data may affect the interpretation, analysis of the fits of the disease models has also provided new insights into the pathogenesis of chronic filarial disease. First, the per capita rate of development of chronic disease (both hydrocele in men and lymphoedema) due to adult worms may increase with transmission intensity, implying that individual worm pathogenicity is positively related to mean worm burden within the host. Although this finding is dependent on adjusting the mf intensity from the low transmission community of Kingwede (Tables 4 and 5), it not only has intuitive biological appeal (damage to the lymphatics can clearly increase as more worms enter the lymphatics), but also has implications for the capacity of mass chemotherapy in reducing long-term filarial morbidity in the community (see below). Given the potential importance of this result, it is clear that it should be reassessed using a more sensitive estimation of infection, perhaps antigen assay tests with no upper OD value cut-offs. More sensitive and standardized estimation of infection from communities in different endemic regions will also be essential if regional differences in worm pathogenicity, as implied by the different disease parameter values in East Africa compared to those in South India (15), are to be evaluated.

The second important finding relates to the relationship between the prevalence of lymphoedema and community transmission intensity. The results suggest that, as transmission intensity increases (at least to the levels studied), the disproportionate effect of worm-induced morbidity will be aggravated by immunopathological reactions. This suggests a nonlinear increase in the rates of both hydrocele and lymphoedema as transmission increases but with a greater increase in observed lymphoedema prevalence (above that due to physical damage by worms) in areas of high transmission because of immunopathology. Evaluation of

this conclusion against parallel data on exposure intensity, infection and disease (3) is difficult given the different methodologies used. This result also suggests that it will be difficult to disentangle worm-induced from immune-induced impacts on lymphoedema prevalence merely from empirical analysis of paired transmission intensity and disease data. The present analysis suggests that this is likely to be resolved only by the use of mechanistic models, such as the one presented here, to analyse and compare standardized field data.

This investigation has also provided intriguing insights into the nature of immunity in filariasis. Although preliminary, the results suggest that there may be distinct patterns of immune response within the same individual that separately influence infection and chronic disease. Thus, while immunity against infection reflects past experience of adult worms acting against the establishment of larvae, the immunopathological component of lymphoedema is apparently more related to cumulative experience of larvae rather than of adult worms. While clearly requiring further investigation, possibly by comparison with data from a community with a higher transmission intensity than Tawalani, this result confirms the complex nature of filarial immunity. It also suggests that analyses of immunological data alone are unlikely to give conclusive insights into the relative contributions of infection- or disease-related immunity. Indeed, the present study indicates a major use of mechanistic models lies in their application directly in the analysis and interpretation of such immunoepidemiological datasets (20).

These results, particularly the idea of transmission intensity-dependent immunity, have important implications for attempts to control filariasis by mass chemotherapy (11). The finding of a positive interaction between transmission intensity and acquired immunity suggests that, to achieve an equivalent reduction in levels of community infection in areas of high transmission, a longer period of treatment than in areas of low to moderate transmission would be required (28). However, it is apparent that this will depend critically on the transmission threshold above which immunity will become significant. By contrast, the implication for treatment to reduce chronic filariasis morbidity is clear. Any reduction in worm load, especially among the younger age groups, may lead to a disproportionate reduction in long-term disease development. Furthermore, this beneficial effect is likely to be even greater in areas of higher transmission because of parallel reductions in transmission and hence disease-inducing immunopathology. A better understanding of the interrelationships between exposure, immune responses and infection/disease patterns will therefore not only lead to improved understanding of basic filariasis

epidemiology, but also of the epidemiological effects of control.

ACKNOWLEDGEMENTS

This study received financial support from the INCO-DC Programme of the European Community (contract no. ERBIC 18 CT 970257) and the Danish Bilharziasis Laboratory, Denmark. EM gratefully acknowledges the Medical Research Council, UK, for Fellowship support.

REFERENCES

- Brunhes J. La filariose de Bancroft dans la sous-region Malgache. *Memoires D'orstom* 1975; **81**: 212.
- Wijers DJB. Bancroftian filariasis in Kenya. IV. Disease distribution and transmission dynamics. *Ann Trop Med Parasitol* 1977; **71**: 451–463.
- Southgate BA. Intensity and efficiency of transmission and the development of microfilaraemia and disease: their relationship in lymphatic filariasis. *J Trop Med Hygiene* 1992; **95**: 1–12.
- Kazura JW, Bockarie M, Alexander N *et al*. Transmission intensity and its relationship to infection and disease due to *Wuchereria bancrofti* in Papua New guinea. *J Infect Dis* 1997; **176**: 242–246.
- Michael E, Bundy DAP. Herd immunity to filarial infection is a function of vector biting rate. *Proc Royal Soc London B* 1998; **265**: 855–860.
- Denham DA, McGreevy PB, Suswillo RR, Rogers R. The resistance to re-infection of cats repeatedly inoculated with infective larvae of *Brugia pahangi*. *Parasitology* 1983; **86**: 11–18.
- Denham DA, Fletcher C. The cat infected with *Brugia pahangi* as a model of human filariasis. *Ciba Foundation Symp* 1987; **127**: 225–235.
- Grenfell BT, Michael E, Denham DA. A model for the dynamics of human lymphatic filariasis. *Parasitol Today* 1991; **7**: 318–323.
- Michael E, Grenfell BT, Isham VS, Denham DA, Bundy DAP. Modelling variability in lymphatic filariasis: macrofilarial dynamics in the *Brugia pahangi*–cat model *Proc Royal Soc London B* 1998; **265**: 155–165.
- Osborne J, Devaney E. The L3 of *Brugia* induces a Th2-polarized response following activation of an IL-4-producing CD4-CD8-T cell population. *Int Immunol* 1998; **10**: 1583–1590.
- Ottesen E, Duke BOL, Karam M, Behbehani K. Strategies and tools for the control/elimination of lymphatic filariasis. *Bull World Health Organ* 1997; **75**: 491–503.
- Bundy DAP, Grenfell BT, Rajagopalan PK. In: Ash C, Gallagher RB, eds. *Immunoparasitology Today*. Cambridge: Elsevier Trends Journals; 1991:A71–A75.
- Grenfell BT, Michael E. Infection and disease in lymphatic filariasis: an epidemiological approach. *Parasitology* 1992; **104**: S81–S90.
- Chan MS, Guyatt HL, Dundy DAP, Medley GF. Dynamic models of schistosomiasis morbidity. *Am J Trop Med Hygiene* 1996; **55**: 52–62.
- Chan MS, Srividya A, Norman RA *et al*. Epifil: a dynamic model of infection and disease in lymphatic filariasis. *Am J Trop Med Hygiene* 1998; **59**: 606–614.
- Anderson RM, May RM. Infectious diseases of humans. *Dynamics and Control*. Oxford: Oxford University Press; 1991.
- Woolhouse MEJ, Taylor P, Matanhire D, Chandiwana SK. Acquired immunity and epidemiology of *Schistosoma haematobium*. *Nature* 1991; **353**: 757–759.
- Fulford AJC, Butterworth AE, Sturrock RF, Ouma JH. On the use of age-intensity data to detect immunity to parasitic infections, with special reference to *Schistosoma mansoni* in Kenya. *Parasitology* 1992; **105**: 219–227.
- Chan MS, Mutapi F, Woolhouse MEJ, Isham VS. Stochastic simulation and the detection of immunity to schistosome infections. *Parasitology* 2000; **120**: 161–169.
- Woolhouse MEJ. A theoretical framework for the immunoepidemiology of helminth infection. *Parasite Immunol* 1992; **14**: 563–578.
- Norman RA, Chan MS, Srividya A *et al*. The development of an age-structured model for describing the transmission dynamics and the control of lymphatic filariasis. *Epidemiol Infect* 2000; **124**: 529–541.
- Simonsen P, Meyrowitsch DW, Jaoko JW *et al*. Bancroftian filariasis infection, disease and specific antibody response patterns in a high and low endemic community in East Africa. *Am J Trop Med Hygiene* 2001; in press.
- McMahon JE, Magayuka SA, Kolstrup N, Mosha FW, Bushrod FM, Abaru DE. Studies on the transmission and prevalence of bancroftian filariasis in four coastal villages of Tanzania. *Ann Trop Med Parasitol* 1981; **75**: 415–431.
- McMahon JE, de Marshall TFC, Vaughan JP, Abaru DE. Bancroftian filariasis: a comparison of microfilariae counting techniques using counting chamber, standard slide and membrane (nucleopore) filtration. *Ann Trop Med Parasitol* 1979; **73**: 457–464.
- Meyrowitsch DW, Simonsen PE, Makunde WH. Bancroftian filariasis: analysis of infection and disease in five endemic communities of north-eastern Tanzania. *Ann Trop Med Parasitol* 1995; **89**: 653–663.
- Nelson GS. The identification of infective filarial larvae in mosquitoes with a note on the species found in wild mosquitoes caught on the Kenya coast. *J Helminthol* 1959; **33**: 233.
- Walsh JF, Davies JB, Le Berre R. Standardization of criteria for assessing the effect of Simulium control on onchocerciasis control programmes. *Trans Royal Soc Trop Hygiene Med* 1978; **72**: 675–676.
- Anderson RM, May RM. Herd immunity to helminth infection and implications for parasite control. *Nature* 1985; **315**: 493–496.
- Ottesen EA. The human filariases: new understandings, new therapeutic strategies. *Curr Opin Infect Dis* 1994; **7**: 550–558.
- Pani SP, Yurraj J, Vanamail P *et al*. Episodic adenolymphangitis and lymphoedema in patients with bancroftian filariasis. *Trans Royal Soc Trop Med Hygiene* 1995; **89**: 72–74.
- World Health Organization. *Report of a Consultative Meeting on the Application of Modelling to Control Strategies in Lymphatic Filariasis*. Geneva: World Health Organization; 1996.
- Freedman DO. Immunopathogenesis of human lymphatic filariasis. *Parasitol Today* 1998; **14**: 229–234.
- Hillborn R, Mangel M. *The Ecological Detective. Confronting Models with Data*. Princeton, NJ: Princeton University Press; 1997.
- McCallum H. *Population Parameters. Estimation for Ecological Models*. Oxford: Blackwell Science Ltd; 2000.
- Park CB. Microfilarial density distribution in the human population and its infectivity index for the mosquito population. *Parasitology* 1988; **96**: 265–271.
- Grenfell BT, Das PK, Rajagopalan PK, Bundy DAP. Frequency

- distribution of lymphatic filariasis microfilariae in human populations: population processes and statistical estimation. *Parasitology* 1990; **101**: 417–427.
- 37 Basanez M-G, Boussinesq M. Population biology of human onchocerciasis. *Phil Transactions Royal Soc London B* 1999; **354**: 809–826.
- 38 McMahon JE, de Marshall TFC, Vaughan JP, Kolstrup N. Tanzania Filariasis Project: a provocative day test with diethyl-carbamazine for the detection of microfilariae of nocturnally periodic *Wuchereria bancrofti* in the blood. *Bull World Health Organ* 1979; **57**: 759–765.
- 39 Meyrowitsch DW, Simonsen PE, Makunde WH. A 16-year follow-up study on bancroftian filariasis in three communities of north-eastern Tanzania. *Ann Trop Med Parasitol* 1995; **89**: 665–675.
- 40 Simonsen PE, Meyrowitsch DW. Bancroftian filariasis in Tanzania: specific antibody responses in relation to long-term observations on microfilaremia. *Am J Trop Med Hygiene* 1998; **59**: 667–672.
- 41 Plaisier AP, Subramanian S, Das PK *et al.* The LYMFASIM simulation programme for modelling lymphatic filariasis and its control. *Meth Inform Med* 1998; **37**: 97–108.